UDC 539.4

Optimization of Residual Stresses in Laser-Mixed WC(Co,Ni) Coatings

C. W. Liu,[a] M. D. Jean,[a,1] Q. T. Wang,[b] and B. S. Chen[a]

[a] School of Mechanical and Automotive Engineering, Laboratory of New Materials Preparation and Forming Technology, Fujian University of Technology, Fuzhou, China

[b] School of Materials Science and Engineering, Fujian Provincial Key Laboratory of New Materials Preparation and Forming Technology, Fujian University of Technology, Fuzhou, China

[1] mdjeam@foxmail.com

A ternary mixture of tungsten carbide (WC), cobalt (Co), and nickel (Ni) powders is prepared to form ceramic-metal composite coatings employed for laser cladding of 40Cr steel. This coating is investigated using the mixture design to evaluate the influence of its ratios on the residual stresses in the clads. The WC/Co/Ni ternary mixture exhibits higher residual stresses than those of the Co/Ni or WC/Ni binary mixtures, except for the WC/Co one. Single WC, Co, or Ni designs illustrate a high sensitivity of residual stresses, cracks pass through the interior of WC particles rather than around them, and the cracks mostly propagate along the eutectic phases at 50%Co–50%WC. A reduced special quartic model in the mixture design exhibits excellent fit, predicted and experimental values of residual stresses for these laser clads are in good agreement.

Keywords: tungsten carbide, mixture, reduced special quartic model, residual stress optimization.

Introduction. Tungsten carbide composite coatings, which are widely used as coatings in hardfacing applications, have been the subject of much study as an alternative to traditional hardfacing materials in additive manufacturing industries. Due to their unique solid solution hardening properties, these coatings produce high hardness, wear resistance and corrosion resistance for use in cutting tools, turbine blades, engine valves and other wear-resistant components [1–3]. Accordingly, tungsten carbide composite materials have great industrial importance as advanced ceramic materials for powder-based hardfacing. Despite their high hardness, high melting point and thermodynamic stability, they have several shortcomings, such as inhomogeneous distribution, thermal stress concentration and susceptibility to cracks, especially in high volume fraction WC coatings [4–6]. These defects influence the mechanical properties of the coating in applications for cladding WC welds. Recently, numerous powder-based techniques using ceramic materials have been proposed that are capable of producing complex geometries, as well as close adherence to their net-shape [7–10]. Laser cladding has superior properties over and above previously properties and several advantages over conventional hardfacing techniques, including dense features, metallurgical bonding to the substrate, lower distortion, manufacturing flexibility and non-porous structure. It is a vital powder-based technology for the production of protective coatings that can resist specific environments. However, there are few studies of residual stress for ternary mixtures of WC/Co/Ni powders that form composite WC/Ni/Co cladding using different proportions of powders during laser cladding. WC–Co or –Ni or –Co/Ni coatings have been studied, but these studies mostly focus on process-induced residual stresses for laser cladding-clad welds [11–16]. In order to relax thermal stress, a simplex-centroid design addresses the problem of using three powders in different proportions, and it allows better control of the mixtures for laser-welded cladding. This method can provide a detailed picture of the microstructural evolution, crack behavior, and residual stresses.

© C. W. LIU, M. D. JEAN, Q. T. WANG, B. S. CHEN, 2019

This study uses a response surface methodology with a simplex-centroid mixture to determine the effect of a three-component mixture, in which residual stress is optimized. The influence of different mixture ratios and mixtures of the three-component alloys on residual stress distribution and microstructural evolution is analyzed in the laser WC/Co/Ni composite clads.

1. **Experimental**.

1.1. ***Materials and Preparations***. The fiber laser cladding system consists of an IPG YLS-3000 fiber laser, a 6-axis robot, an inductive power source, a computer numerical controller and a powder feeder (HUST III). An IPG fiber laser with a maximum power of 3000 W and wave length of 1.07 μm was used. Parameters and conditions of mixed WC, Co, and Ni clads by laser cladding are shown in Table 1. The WC/Co/Ni blends were composed of WC, Co, and Ni powders with sizes of 125 to 300 lm, a WC composition of 90 wt.% W, 10 wt.% C and the balance of Ni and Co. The WC/Co/Ni blends were coaxially fed into the laser-induced melt pool through a coaxial nozzle. To determine the optimal combination of these ingredients, three different alloy powder compounds were blended for the laser clad: X_1 (A = WC), X_2 (B = Co), and X_3 (C = Ni). The substrate metal was 40Cr steel with dimensions of 40, 20, and 10 mm. The working surface was cleaned using absolute ethyl alcohol. To understand the morphologies of the composite deposits, crack morphology and element distribution in the coatings were examined by scanning electronic microscope (SEM) with a EDS analysis, the Hitachi S-2600H (Tokyo, Japan). The specimens were chemically etched in a mixed acid including 80 vol.% HCl and 20 vol.% HNO_3 for 20–30 s. A residual stress analysis at the bead centerline is estimated using an XRD diffractometer (Proto iXRD) with the $\sin 2\psi$ method [6]. The data and the control factors, as well as levels in the coded design units are shown in Table 2. The crack behavior and fractures due to residual stress were studied, as well as relationships between the three-component mixtures and the residual stress for the laser clads.

Table 1

Parameters and Conditions of Mixed WC, Co, and Ni Clads by Laser Cladding

Symbol	Substrate	Laser power (W)	Powder feed rate (1/min)	Stand-off distance (mm)	Scanning speed (mm/s)
H1	40 Cr	1200	1500	20	8

Table 2

Element Analysis of the Preparation of Additive in WC (Co,Ni)

No.	C	O	S	Fe	Co	Ni	Cu	W	Location
2	3.215	1.708	0.123	1.885	0.161	0.197	0.294	92.770	*A*
10	4.054	12.686	0.430	7.765	4.699	4.862	0.172	65.330	*B*
4	1.464	6.642	0.108	2.403	0.515	22.510	0.286	66.052	*C*
7	1.679	1.111	0.077	0.951	22.266	1.000	0.425	72.490	*D*

1.2. ***Mixture Design***. A mixture design is a special type of response surface experiment in which the factors are the ingredients of a mixture and the response is a function of the proportions of each ingredient [12]. Three parameters with WC (x_1), Co (x_2), and Ni (x_3) elements represent the proportions by weight of the three powder materials. The form of the polynomial model is used to fit to data from a mixture experiment. In general, the standard forms of the mixture models in the simplex-centroid design are as follows:

$$E(y)=\sum_{i=1}^{n}\beta_i x_i+\sum\sum_{i<j=2}^{n}\beta_{ij}x_i x_j+\sum\sum\sum_{i<j<k=3}^{n}\beta_{ijk}x_i x_j x_k. \quad (1)$$

A {3, 3} simplex lattice design is used to study the laser clads, which are composed of several alloy powders, such as WC, Co, and Ni, that are blended to form laser clads. By minimizing the sum of squared errors. The regression coefficients β are determined.

2. **Results and Discussion**.

2.1. ***Residual Stress***. The surface residual stresses for 100% WC as determined by X-ray diffraction are performed from the combination of the three different ingredients, as shown in Fig. 1, which shows the residual stress for the clads, as derived from the slope of the plot of lattice spacings against $\sin 2\psi$, and fitting a Gaussian function to a measured peak from the X-ray diffraction results in Fig. 1a, to calculate the residual stresses. In all cases, the distribution of the measured residual stresses ranges from −231.21 to 137.0 MPa with mixture different proportions for the laser clads, which are between a compressive stress and a tensile stress. As shown in Fig. 1b–d, the variation and the amount of residual

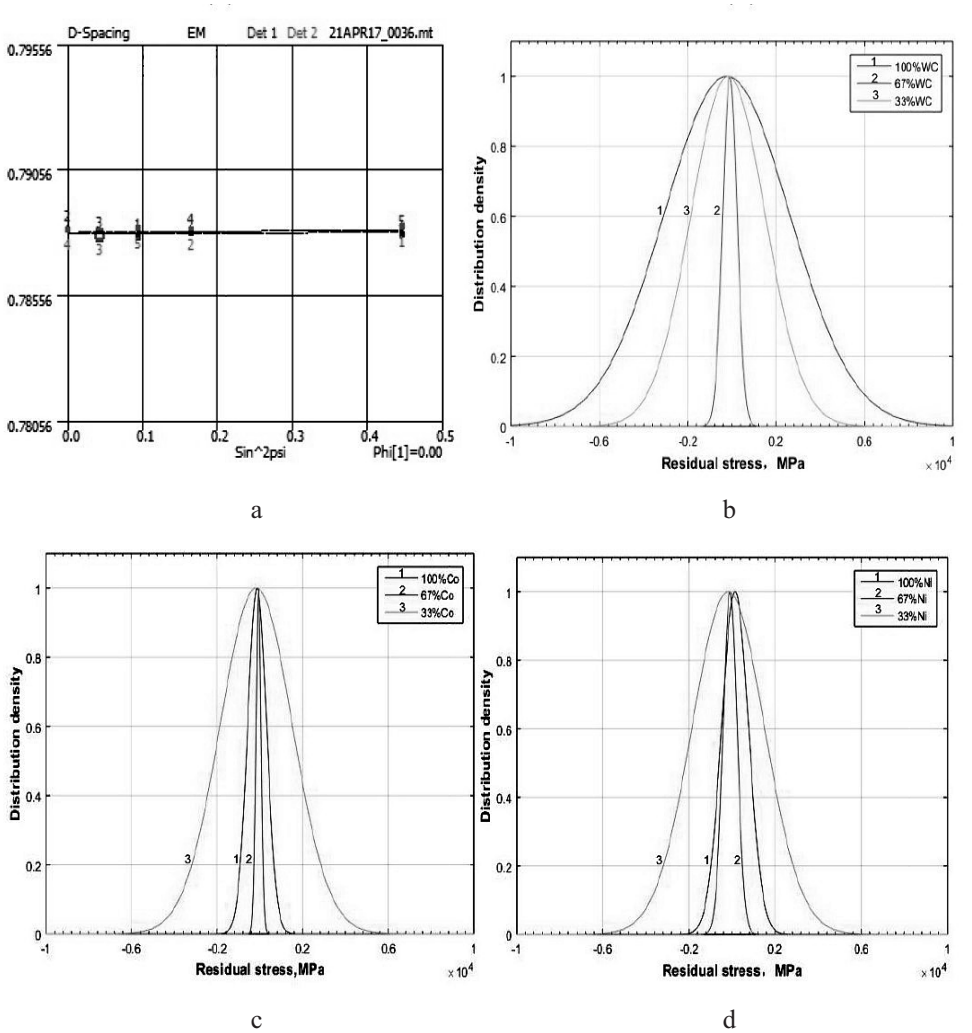

Fig. 1. The measured residual stresses of the pattern of fitting a Gaussian function to a measured peak by X-ray diffraction.

stress for both 100% WC and 100% Co are −231.21 MPa (Fig. 1b) and −136.52 MPa (Fig. 1c), respectively, which correspond to compressive stress range, while 100% Ni has a tensile stress of 137.0 MPa (Fig. 1d). This behavior is mainly due to the multiple variations in the microstructure and phases, the proportions of the mixtures, the processing parameters and thermal expansion in the clads. In all the trials, markedly lower residual stresses are recorded, except for the single alloy of 100% WC or 100% Co or 100% Ni, for trial 1 with a mixture of 33.33% WC, 33.33% Co, and 33.33% Ni, and for trial 7 with a mixture of 50% WC and 50% Co. When the proportion of WC is increased, the compressive stress and cracking increase significantly, so the high proportion of WC alloy that is mixed with Co and Ni contents has a significant effect on the sensitivity to cracking due to high residual stresses.

2.2. ***Microstructure Evolution***. Figure 2a and Table 2 show that the morphology of conventional 100% WC in trial 2 exhibits a white dendritic area with a dark bonding line at the coating/substrate interface. The microstructures consist mainly of several dendritic WC-rich solid solutions, metallurgical faults and some unmelted WC particles, shown as *A* in Fig. 2a. These have W contents of 92.77 wt.%. The high degree of unmelted WC particles exists in the molten zone. The brittle phases of unmelted WC particles with high stress concentration may cause the regeneration of cracks during solidification. For WC contents of 66.67% in trial 10, the solidified zone of molten 16.67% Co/Ni elements is surrounded by WC particles that form heterogeneous structural growths during laser cladding. Additionally, several partially melted WC particles are preferentially dissolved to form free W and C atoms that diffuse into the molten zone, forming nanocarbide eutectics around WC particles, marked as *B*. These include 65.33% WC with fewer 12.686% O elements in Fig. 2b. As shown in Fig. 2c, the content of WC particles in trial 4 is 50% and there is partial melting of WC particles, as clearly shown by the sharp edges of the WC, because of the relatively high solubility of Ni particles at 50% in the molten zone and the uniform dispersion of the molten WC that is formed marked as *C* during cladding welds. The molten zone with Ni particles at 22.51 wt.% that separates the small carbide particles is uniformly distributed due because the molten Ni-based alloys have good wettability. The grain refinement of precipitated carbides hinders crack initiation and reduces the susceptibility to cracking. These formations reduce susceptibility to cracking. As Fig. 2d shows, when the content of WC particles in trial 7 is 50%, unmelted WC particles and metallurgical faults such as cracks and gas porosity are not found when the Co composition is 50%. Here there is a continuous Co-based structure that separates the carbides, in which fine grains of cobalt are uniformly distributed and marked as *D*. No pores are formed, so there is a fairly homogeneous structure. This decreases the surface energy that is available in the molten area and reduces the nucleation of cracks and crack propagation. As seen in the EDS analysis results above, If the amount of WC elements increase, dendrites and eutectics with crack initiation and propagation are markedly generated. Thus, cracks of high brittle fractures in the unmelted WC particles are easily found, so the brittle carbide adjoining high stress can make the clad more susceptible to cracking.

2.3. ***Empirical Models of the Response Surfaces***. All of the residual stresses for the XRD data are analyzed using SPSS20, a widely-used software package that supports regression, experimental design and RSM. The simplex-centroid design for three components is used to study the residual stress for laser clads. It is concluded that the special quadratic terms are significantly more accurate for predicting the responses than others, such as first-order and interaction models because the p-value < 0.05. The canonical forms of the mixture model for laser cladding process are used and the reduced special quartic mixture (Y_1), is selected as follows:

$$Y_1 = -221.78A - 132.81B +$$

$$+123.88C - 35.75AB + 426.21AC + 410.24BC - 1537.41ABC^2. \quad (2)$$

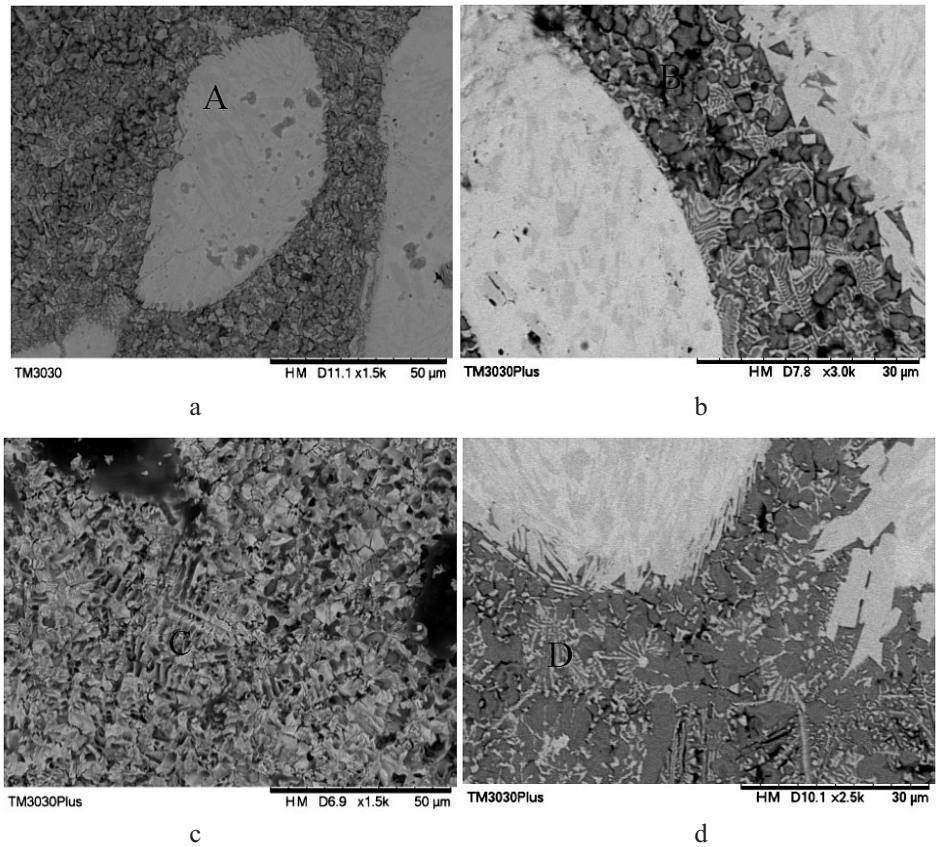

Fig. 2. SEM features of adding Co/Ni alloys to WC power with various mixed designs by laser cladding including (a) trial 2, (b) trial 10, (c) trial 4, and (d) trial 7.

2.4. ***Effect of Mixture Ratio of WC/Co/Ni on Residual Stress***. The fitted models for the canonical forms of the mixture model are constructed using Eq. (2) and contour plots for the predicted response, and the optimal proportions of WC, Ni, and Co blends are determined. Figure 3 shows the triangular response surface with contour plots to show the effect of mixed WC, Ni, and Co on residual stress for the laser-clad welds that are generated by a reduced special quartic mixture. The response plot shows a decrease in residual stress yield when Co concentration increases. The residual stress yield increases as the WC concentration increases. However, the contours produce different hypsographic map regions and changes in the color of surface contour mapping regions show the variations of the residual stress responses. The optimum zone of 50–70% WC, 0–20% Co, and 20–40% Ni gives the least residual stress for the WC/Co/Ni blend in the mixture design. The green area near the zero line shows the ideal residual stress. Overall, similar results are visible for various models. Only the predictive curves with desired values are different. That is, the predicted and measured responses have different levels of accuracy for three models. Clearly, the decrease in residual stress is due to the addition of proper amounts of Ni element into the WC/Ni/Co blends, but this stress increases when the amount of WC powders increase. The figures show a contour region for the reduced special quartic mixture that demonstrates a lower residual stress of 37.92 MPa, and a blend of 56.67% WC, 39.17% Ni, and 4.17% Co was chosen of 57% WC, 39% Ni, and 4% Co. The regions of the triangular contour plots with green highlights have the desired values for individual and mixture components on the residual stress pattern and also have more effect

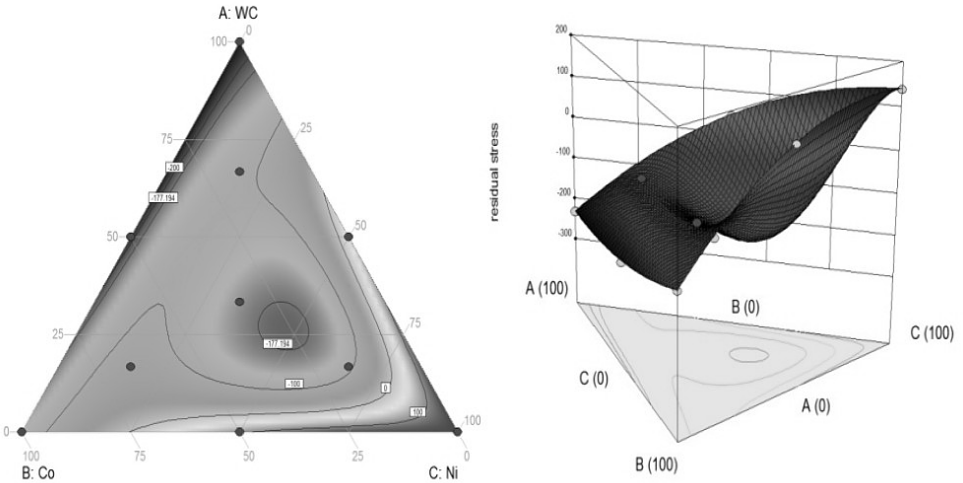

Fig. 3. Triangular contour plots for powder mixed effects for a reduced special quartic mixture, accounting for the effect of individual and mixture powder components including WC, Ni, and Co for the residual stresses. The red solid dots on the contour plot are the design points.

on the output than the region of other highlights, for different combinations of mixture components in the laser-clad welds.

Conclusions. As a result of the laser-clad welds, a homogeneous microstructure is obtained by adding Co/Ni alloys to WC in the molten zones, and gas porosity, microcracks and intermetallic defects in the single WC are visible. The cracks pass through WC particles, rather than around them at 100% WC, whereas the cracks mostly propagate along the eutectic phases at 50% Ni–50% WC. Additionally, the WC/Co/Ni ternary mixture exhibits higher residual stress than that of the Co/Ni binary mixture or the WC/Ni binary mixture, except for the 50% WC–50% Co binary mixture, where a tendency to cracking in the ternary mixture is not apparent. Meanwhile, single WC, Co, or Ni contents exhibit a great tendency for cracking. Furthermore, the reduced special quartic mixture is significantly more accurate for forecasting residual stress responses than the linear mixture or the quadratic mixture models. Detailed examination of the triangular contour plots shows that a lower residual stress of 37.92 MPa and a blend of 57% WC, 39% Ni, and 4% Co contents are obtained. This blend significantly reduces the susceptibility to cracking, and cracking is not easily induced in the laser clads.

Acknowledgments. This work was financially supported by the Foundation of Fujian Provincial Education Department China (Grant Nos. JA14208, JA14216).

1. P. Wen, Z. Feng, and S. Zheng, “Formation quality optimization of laser hot wire cladding for repairing martensite precipitation hardening stainless steel,” *Opt. Laser Technol.*, **65**, 180–188 (2015).
2. D. Shu, Z. Li, C. Yao, et al., “In situ synthesised WC reinforced nickel coating by laser cladding,” *Surf. Eng.*, **33**, No. 4, 276–282 (2017).
3. B. M. Dhakar, D. K. Dwivedi, and S. P. Sharma, “Studies on remelting of tungsten carbide and rare earth modified nickel base alloy composite coating,” *Surf. Eng.*, **28**, No. 1, 73–80 (2012).
4. C. Wang, C. Jiang, and V. Ji, “Thermal stability of residual stresses and work hardening of shot peened tungsten cemented carbide,” *J. Mater. Process. Tech.*, **240**, 98–103 (2017).

5. D. Shu, Z. Li, K. Zhang, et al., "In situ synthesized high volume fraction WC reinforced Ni-based coating by laser cladding," *Mater. Lett.*, **195**, 178–181 (2017).
6. Q. Luo and A. H. Jones, "High-precision determination of residual stress of polycrystalline coatings using optimised XRD-sin 2ψ technique," *Surf. Coat. Tech.*, **205**, No. 5, 1403–1408 (2010).
7. T. Mukherjee, W. Zhang, and T. DebRoy, "An improved prediction of residual stresses and distortion in additive manufacturing," *Comp. Mater. Sci.*, **126**, 360–372 (2017).
8. M. L. Zhong, W. J. Liu, K. F. Yao, et al., "Microstructural evolution in high power laser cladding of Stellite 6+WC layers," *Surf. Coat. Tech.*, **157**, Nos. 2–3, 128–137 (2002).
9. K. Zhang, J. Deng, Y. Xing, et al., "Periodic nano-ripples structures fabricated on WC/Co based TiAlN coatings by femtosecond pulsed laser," *Surf. Eng.*, **31**, No. 4, 271–281 (2015).
10. M. Afzal, A. N. Khan, T. B. Mahmud, et al., "Effect of laser melting on plasma sprayed WC-12 wt.%Co coatings," *Surf. Coat. Tech*., **266**, 22–30 (2015).
11. U. de Oliveira, V. Ocelik, and J. Th. M. De Hosson, "Residual stress analysis in Co-based laser clad layers by laboratory X-rays and synchrotron diffraction techniques," *Surf. Coat. Tech.*, **201**, Nos. 3–4, 533–542 (2006).
12. R. H. Myers, D. C. Montgomery, and C. M. Anderson-Cook, *Response Surface Methodology: Process and Product Optimization Using Designed Experiments*, John Wiley & Sons, New York (2009).
13. B. T. Lin, M. D. Jean, and J. H. Chou, "Using response surface methodology for optimizing deposited partially stabilized zirconia in plasma spraying," *Appl. Surf. Sci.*, **253**, No. 6, 3254–3262 (2007).
14. Y. Rostamiyan, A. Fereidoon, A. G. Ghalebahman, et al., "Experimental study and optimization of damping properties of epoxy-based nanocomposite: Effect of using nanosilica and high-impact polystyrene by mixture design approach," *Mater. Design*, **65**, 1236–1244 (2015).
15. N. S. Pillai, P. S. Kannan, S. C. Vettivel, and S. Suresh, "Optimization of transesterification of biodiesel using green catalyst derived from Albizia Lebbeck Pods by mixture design," *Renew. Energ.*, **104**, 185–196 (2017).
16. S. F. Zhou, J. B. Lei, X. Q. Dai, et al., "A comparative study of the structure and wear resistance of NiCrBSi/50 wt.% WC composite coatings by laser cladding and laser induction hybrid cladding," *Int. J. Refract. Met. H.*, **60**, 17–27 (2016).

Received 15. 03. 2018